














Salivary gland adenocarcinoma in a capuchin monkey (*Sapajus nigritus*)¹

Alessandra da Cruz² , Crisan Smaniotto³ , Vinicius Dahm² ,
Amália Ferronato² , Manoela M. Piva^{2*} , Nelson D. Lucas⁴ ,
Luana Canavessi² , Laura F. de Noronha² , Marilene M. Silva² ,
Flávio S. Jojima²  and Aline M. Viott² 

ABSTRACT.- Da Cruz A., Smaniotto C., Dahm V., Ferronato A., Piva M.M., Lucas N.D., Canavessi L., De Noronha L.F., Silva M.M., Jojima F.S. & Viott A.M. 2025. **Salivary gland adenocarcinoma in a capuchin monkey (*Sapajus nigritus*)**. *Pesquisa Veterinária Brasileira* 45:e07580, 2025 Departamento de Ciências Veterinárias, Universidade Federal do Paraná, Setor Palotina, Rua Pioneiro, 2153, Palotina, PR 85950-000, Brazil. E-mail: manoela.marchezan@gmail.com

Salivary gland neoplasms are infrequently documented in veterinary medicine and rare in non-human primates; therefore, they are scarce in the literature. Adenocarcinomas are malignant neoplasms that originate in the glandular epithelium and can affect various species. Our study presents detailed cytological, histological, and immunohistochemical findings of a salivary gland adenocarcinoma in a capuchin monkey (*Sapajus nigritus*). In the necropsy, a multilobulated mass was observed in the left submandibular region, characterized by a dark red surface, soft and firm upon cut surface. Histologically, a neoplastic proliferation of malignant epithelial cells was identified in the submandibular region and the lungs. The cells showed acinar formation, areas of architectural tissue differentiation loss, and solid aggregates. Immunohistochemistry was conducted to corroborate and elucidate the case. In the neoplasia, there was positive immunolabelling for pan-cytokeratin (Pan CK) and cytokeratin 7 (CK7), and negative labeling for thyroglobulin, thyroid transcription factor-1 (TTF-1), cytokeratin 20 (CK20), and Napsin A. The cytological, anatomopathological, and immunohistochemical findings lead to the diagnosis of salivary gland adenocarcinoma. Remarkably, this report seems to be the inaugural documentation of this neoplasm in a capuchin monkey (*Sapajus nigritus*).

INDEX TERMS: Immunohistochemistry, non-human primates, neoplasm, salivary gland adenocarcinoma.

RESUMO.- [Adenocarcinoma de glândula salivar em macaco-prego (*Sapajus nigritus*).] Neoplasias de glândula salivar são pouco documentadas na medicina veterinária e raras em primatas não-humanos, portanto são escassos na literatura. Adenocarcinomas são neoplasias malignas que se originam do epitélio glandular e podem afetar várias espécies. Nosso estudo apresenta achados citológicos, histológicos e imuno-histoquímicos de um adenocarcinoma de glândula salivar em macaco-prego (*Sapajus nigritus*). Na necropsia, foi

observada uma massa multilobulada na região submandibular esquerda, caracterizada por uma superfície vermelha escura e macia a firme ao corte. Histologicamente, uma proliferação neoplásica de células epiteliais malignas foi identificada na região submandibular e nos pulmões. As células apresentaram formação acinar, áreas com perda de diferenciação tecidual e agregados sólidos. Foi realizado imuno-histoquímica para corroborar e elucidar o caso. Houve imunomarcagem positiva para citoqueratina (Pan CK) e citoqueratina 7 (CK7), e marcação negativa para tireoglobulina, fator de transcrição de tireoide-1 (TTF-1), citoqueratina 20 (CK20) e Napsin A. Os achados citológicos, anatomopatológicos e imuno-histoquímicos levam ao diagnóstico de adenocarcinoma de glândula salivar. Este relato apresenta um caso que parece ser inédito desta neoplasia em um macaco-prego (*Sapajus nigritus*).

TERMOS DE INDEXAÇÃO: Imuno-histoquímica, primatas não-humanos, neoplasia, adenocarcinoma de glândula salivar.

¹Received on January 14, 2025.

Accepted for publication on February 19, 2025.

²Departamento de Ciências Veterinárias, Universidade Federal do Paraná (UFPR), Setor Palotina, Rua Pioneiro 2153, Palotina, PR 85950-000, Brazil.

*Corresponding author: manoela.marchezan@gmail.com

³Prontovet Veterinária, Rua Vitória 1429, Cascavel, PR 85802-229, Brazil.

⁴Departamento de Medicina e Cirurgia Veterinária, Universidade Federal de Minas Gerais (UFMG), campus Pampulha, Av. Antônio Carlos 6627, Belo Horizonte, MG 31270-901, Brazil.

INTRODUCTION

Salivary glands are responsible for producing saliva and can be found in various locations on the head and neck. They have many functions, such as lubricating the oral cavity, moistening food, and initiating digestion due to digestive enzymes in the saliva (Porcheri & Mitsiadis 2019). The salivary glands are divided into major (parotid, submandibular and sublingual) and minor, distributed along the larynx, pharynx, oral cavity, and palatine tonsil (Ogawa et al. 2008). The salivary glands can undergo various alterations, such as sialoadenitis, sialoceles, calculi, infarcts, as well as primary or secondary neoplasms (Spangler & Culbertson 1991, Lieske & Rissi 2020).

Salivary gland neoplasms can occur in several species but are uncommon in veterinary medicine and rare in non-human primates (NHP) (Miller 2012). They can be benign or malignant, and either originate from tubular or ductular epitheliums or have an associated epithelial and mesenchymal component (Zachary 2016). The majority tend to be of epithelial origin, both in humans and other animals (Speight & Barrett 2002, Meuten 2017). Thus, the present study aims to report a case of salivary gland adenocarcinoma in a capuchin monkey (*Sapajus nigritus*).

CASE REPORT

Ethical approval. The person responsible assigned the Donation Agreement at the Veterinary Hospital of Palotina. The data are available and can be accessed upon request from the corresponding author.

A male capuchin monkey (*Sapajus nigritus*), approximately 32 years old, was sent to the Veterinary Pathology Laboratory at the “Universidade Federal do Paraná” (UFPR) for a necroscopic examination. The animal had been under the care of a *bona fide* depositary for approximately 20 years and had a history of multiple nodules in the submandibular region that extended to the cervical region, as well as dysphagia and anorexia. The animal was admitted to a veterinary clinic, sedated with diazepam, and referred to the “Universidade Federal do Paraná” (UFPR) Veterinary Hospital.

The physical examination was difficult, as the animal was sedated. Lung crackles and muffled heart sounds were heard. The radiographic examination revealed multiple nodules in the left submandibular and cervical regions, characterized by soft tissue radiopaque structures. Additionally, a small amount of pleural effusion and areas of alveolar lung opacity were noted, suggesting early-stage pneumonia. Abdominal ultrasound showed lesions compatible with chronic nephropathy. The animal's blood count showed a hematocrit of 40% (45 – 53%), leukocytosis of 24,500 cells/ μ L (5,000 – 24,000 cells/ μ L) with neutrophilia and hypoproteinemia of 5.2 g/dL (7.5 – 8.7 g/dL) (Cubas et al. 2014).

Fine-needle aspiration cytology of the submandibular tumor mass was performed *ante mortem*, and the slides were subsequently stained with Diff-Quik. Neoplastic epithelial cells arranged in cohesive clusters, occasionally forming small acini, were observed. The observed cells exhibited a spectrum of morphologies ranging from cuboidal to polygonal shapes, with moderate cytoplasm and indistinct cytoplasmic borders and slightly bluish, sometimes containing fine vacuoles. The nucleus displayed variation from round to oval, central to paracentral, with loose, slightly granular chromatin and

one to six evident nucleoli. Notably, there was prominent anisocytosis and anisokaryosis, along with numerous cells exhibiting karyomegaly and macrocytosis (approximately 10 in 2.37 mm²). A discreet number of multinucleated cells (up to six nuclei) (approximately 10 in 2.37 mm²) was also present. Noteworthy is the absence of mitotic figures in the scrutinized cytological slides. There was a slight number of neutrophils and a substantial population of red blood cells, indicative of blood contamination. Pleural effusion was collected, and the cytology analysis was similar to that described in the submandibular mass (Fig.1). Both suggested malignant epithelial neoplasia. Due to the unfavorable clinical condition and reserved prognosis, we opted for euthanasia and subsequent necroscopic examination.

During the necropsy, a large multilobulated mass was identified in the left submandibular region, causing lateral displacement of the trachea and esophagus to the right and extending into the left ventral cervical region. The mass measured 12.5 x 11.5 x 10.5 cm, with a dark red external surface and a moderate amount of surrounding adipose tissue associated with its capsule (Fig.2). Upon sectioning, the tumor exhibited a heterogeneous pattern, ranging from soft to firm consistency, with a whitish interior interspersed with multifocal to coalescing dark red areas.

In the lung, areas of atelectasis were observed in the cranio-ventral region, associated with multifocal emphysema (Fig.3). No changes suggestive of metastasis were grossly observed. Furthermore, fat degeneration in the liver and diffuse and moderate enlargement of the prostate (prostatic hyperplasia) was observed.

Fragments of all organs, including the neoplasm, were stored in a 10% formalin solution. The fragments were cleaved and processed for histopathology, then embedded in paraffin, cut into 3-5 micrometer sections, and stained using the hematoxylin and eosin (HE) technique.

In the microscopic examination of the submandibular mass, a neoplastic proliferation characterized by a high density of epithelial cells, well-demarcated, poorly encapsulated and with expansive growth was noted. The cells exhibit cuboidal to polyhedral format, arranged in an acinar pattern, forming small and large acini covered by one to two cell layers (Fig.4). Periodically, the neoplastic cells obliterated the acinar lumen, forming solid aggregates with loss of glandular differentiation (Fig.5). These structures were separated by a slight to moderate amount of fibrous connective tissue and small blood capillaries (discrete fibrovascular stroma). The cytoplasm was moderately eosinophilic, with distinct cytoplasmic borders that were poorly evident. The nuclei were paracentral, rounded to oval, with loose chromatin and one to five evident nucleoli. Anisocytosis and anisokaryosis were prominent, with eight mitotic figures observed in 2,37 mm². Additionally, moderate multifocal areas of hemorrhage and necrosis were identified interspersed between the neoplastic cells.

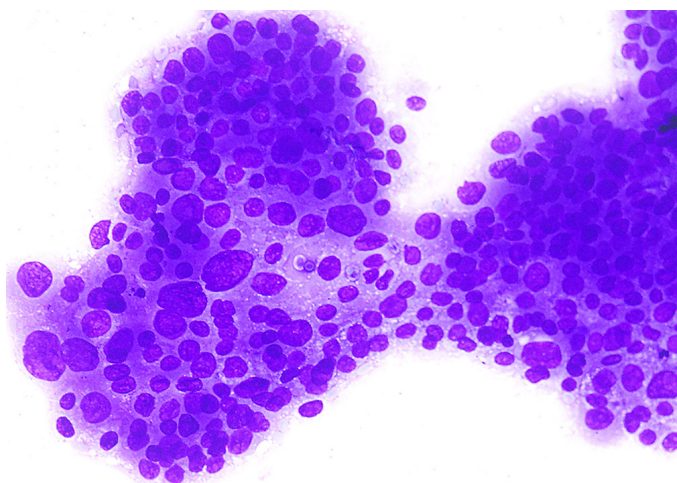
In lung histology, an infiltrate of neoplastic cells similar to those described in submandibular masses was observed within blood vessels and interalveolar septa. These cells exhibited vascular microinvasion, manifested by the disruption of the contiguous basement membrane, thereby defining micrometastases (Fig.6). Concurrently, a predominantly neutrophilic inflammatory infiltrate was found within the airways in a moderate and multifocal to coalescent manner;

particularly evident in the cranial and medial lobes (suppurative bronchopneumonia). In the other organs, notable findings included moderate diffuse prostatic hyperplasia, diffuse and moderate hepatic lipid degeneration, and lymphoplasmacytic interstitial nephritis associated with discreet proliferation of interstitial fibrous connective tissue, with occasional sclerotic glomeruli and membranous glomerulonephritis (findings compatible with chronic kidney disease).

The cytological and histological changes observed were compatible with malignant epithelial neoplasia. The anatomical site of the neoplasm suggested a potential thyroid carcinoma or salivary gland carcinoma; however, the left lobe of the thyroid

was not identified during necropsy, and only a fragment of the submandibular gland was observed.

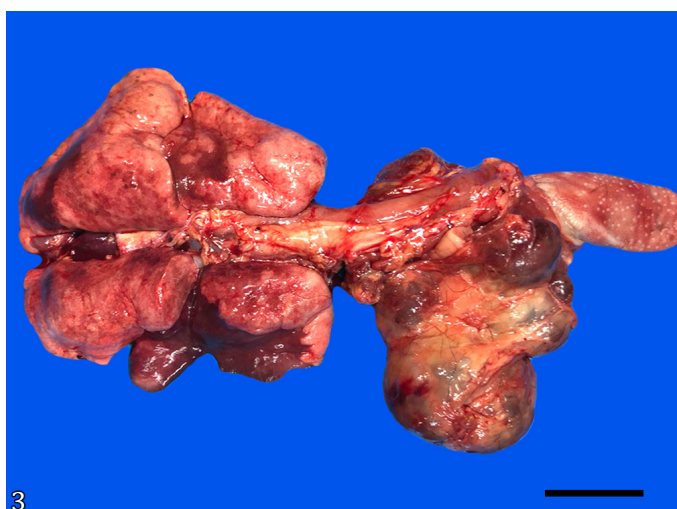
Immunohistochemistry (IHC) was employed to characterize the neoplastic origin of the submandibular nodule. The antibodies used were thyroglobulin (polyclonal), TTF-1 (8G7G3/1, monoclonal), CK7 (OV-TL12/30, monoclonal), Pan CK (AE1AE3, monoclonal), Napsin A (BC15, monoclonal), and CK20 (Ks20.8, monoclonal). All the antibodies are from the Agilent Dako brand and ready-to-use, except for Napsin A (Biocare Medical with dilution; dilution 1:50). All samples with four micrometers histochemical sections were deparaffinized in xylene, hydrated in decreasing concentrations of ethanol, and washed in distilled water. They were then subjected to



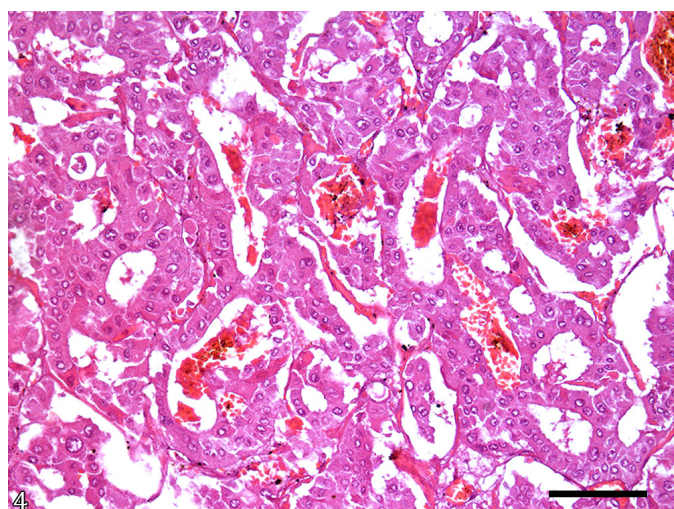
1
Fig.1. Pleural effusion. The figure shows neoplastic epithelial cells arranged in cohesive groups (clusters). They are polygonal to cuboidal, with a round to oval nucleus, moderately bluish and slightly granular cytoplasm. The cells have sharp anisocytosis and anisokaryosis. Diff-Quik stain, bar = 85 μ m.



2
Fig.2. Salivary gland adenocarcinoma, capuchin monkey (*Sapajus nigritus*). Neoplastic proliferation in the left submandibular region, extending to the medial line. It has a multilobulated, delimited appearance with soft to firm consistency, measures 12.5 x 11.5 x 10.5 cm, and is dark red. Bar = 3.5 cm.



3
Fig.3. Neoplastic proliferation laterally displacing the trachea and esophagus; in the lung, there are areas of emphysema, as well as multifocal reddish and depressed cranioventral areas (atelectasis). Bar = 5 cm.



4
Fig.4. Salivary gland adenocarcinoma, capuchin monkey (*Sapajus nigritus*). Submandibular mass: neoplastic proliferation of cuboidal to polyhedral epithelial cells showing acinar arrangement, separated by a discrete fibrovascular stroma. Areas of hemorrhage are also observed. HE, bar = 200 μ m.

antigen retrieval by heat in a high pH solution (Target Retrieval solution High pH-DM828, K800221-2 EnV FLEX+, High pH Link, DAKO) in a pressure cooker (Pascal®, Dako). Afterward, the slides were cooled at room temperature for 20 minutes and washed with deionized water. Endogenous peroxidase was blocked by immersing the slides in ready-to-use hydrogen peroxide (EnVision™ Flex peroxidase-blocking reagent SM801, K800221-2 EnV FLEX+, High pH Link, DAKO). The sections were then washed in Tris solution (pH 7.4). The non-specific sites were blocked with a non-specific reaction-blocking solution (protein block serum-free – DAKO, X0909). Incubation with the primary antibody was performed for 18 hours at 4 °C. EnVision FLEX/HRP, SM802 (Dako) and diaminobenzidine chromogen (EnVision Flex Dab+Chromogen, DM827, DAKO) were used as the amplification and detection system. The slides were counterstained with Harris haematoxylin. Lung and thyroid tissues from *Sapajus nigritus* were used as positive controls for TTF-1. For the negative controls, the primary antibodies were replaced with Universal Negative Control Serum (Biocare) in tumour sections from all cases.

Immunohistochemistry was used to elucidate the origin of the neoplasm. The CK7 and Pan CK antibodies showed a granular, sharp, and diffuse immunolabelling within the cytoplasm of the neoplastic cells in the assessed sections (Fig.7 and 8), affirming a glandular epithelial origin. Conversely, IHC anti-thyroglobulin, anti-TTF-1 (Fig.9), and anti-Napsin A yielded negative in the analyzed sections, effectively excluding a thyroid origin of the neoplasm. Additionally, the anti-CK20 antibody produced negative results in the evaluated sections.

DISCUSSION

Salivary gland adenocarcinomas are malignant neoplasms of epithelial origin, considered rare in humans (Meuten 2017). In contrast, adenocarcinomas constitute the most prevalent tumor type among other animals, especially dogs and cats (Sozmen et al. 2003, Cray et al. 2020). A retrospective study of humans spanning a decade revealed that, out of 63 cases of salivary gland neoplasms, 76.7% were benign, and 23% were malignant (Ribeiro et al. 2021). In comparison, a canine study identified inflammatory changes in 49.7% and neoplastic lesions, predominantly of malignant epithelial origin, in 20.1% of the 179 cases of salivary gland diseases diagnosed over eight years (Lieske & Rissi 2020).

Salivary gland neoplasms are notably rare in NHP, with limited reports in the literature. According to Howard et al. (2019), only 17 published cases have been documented across various NHP species, with no prior reports in capuchin monkeys (*Sapajus nigritus*). Salivary gland tumors in primates are predominantly observed in rhesus monkeys (*Macaca mulatta*), followed by baboons (*Papio spp.*). Isolated case reports exist for other species, such as chimpanzee (*Pan troglodytes*), one of a bonnet monkey (*Macaca radiata*), and one of a mustached tamarin (*Saguinus mystax*). While benign neoplasm reports outnumber malignant ones, only four cases have presented metastasis, with two to lymph nodes (thoracic and retropharyngeal), one to the lung, and one to both the lymph node and lung (Howard et al. 2019).

The mechanisms for the development of salivary gland neoplasms are not fully understood (Horn-Ross et al. 1997, Ho et al. 2011). In humans, radiation exposure is a significant associated factor, both in head and neck therapies and dental

X-rays (Schneider et al. 1997, Ho et al. 2011, American Cancer Society 2022). Remarkably, two observed cases of rhesus monkeys had a history of previous radiation exposure, suggesting a potential risk factor for NHP (Howard et al. 2019). Advancing age is also a recognized factor in neoplasm development, as corroborated by the elderly status of the subject in this case. This aligns with existing literature indicating an increased risk of neoplasms with age in humans and animals.

Clinical manifestations often include the growth of a mass in the salivary gland region, with some cases incidentally identified during necropsy, especially in free-living animals. Clinical signs can be inapparent or include weight loss,

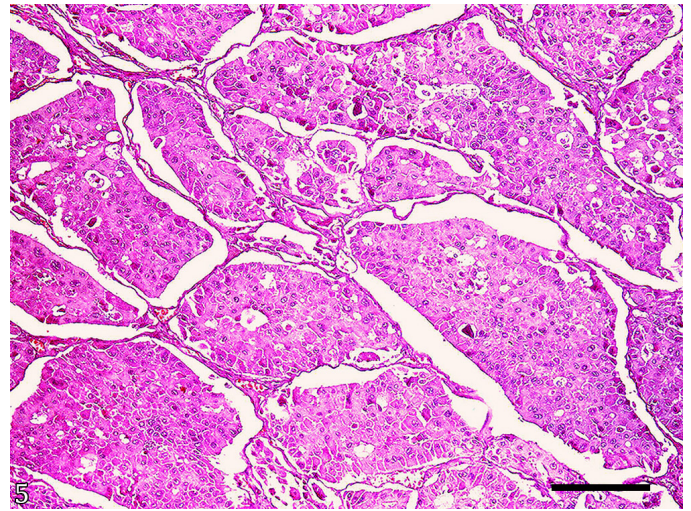


Fig.5. Salivary gland adenocarcinoma, capuchin monkey (*Sapajus nigritus*). Submandibular mass: neoplastic proliferation obliterating the acinar lumen, forming solid aggregates. The cells have moderately eosinophilic cytoplasm, with distinct cytoplasmic borders that are poorly evident. The nuclei are paracentral, rounded to oval, with loose chromatin and one to five evident nucleoli. Anisocytosis and anisokaryosis are prominent. HE, bar = 360 µm.

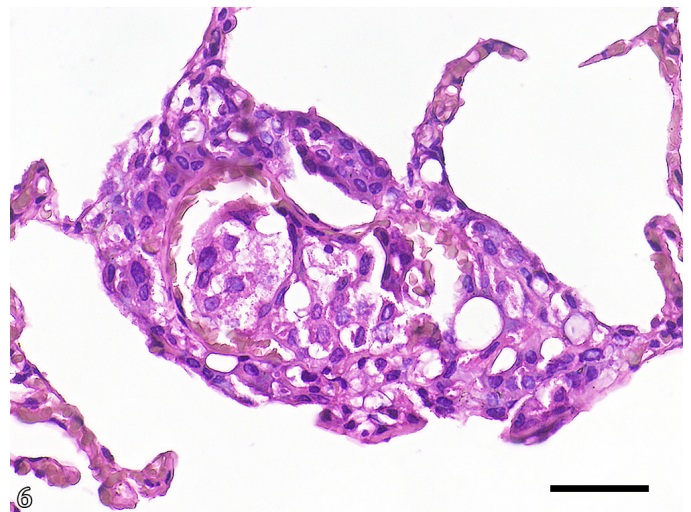


Fig.6. Lung: neoplastic cells in the lumen of blood vessels with disruption of the contiguous basement membrane characterizing a micrometastasis. HE, bar = 85 µm.

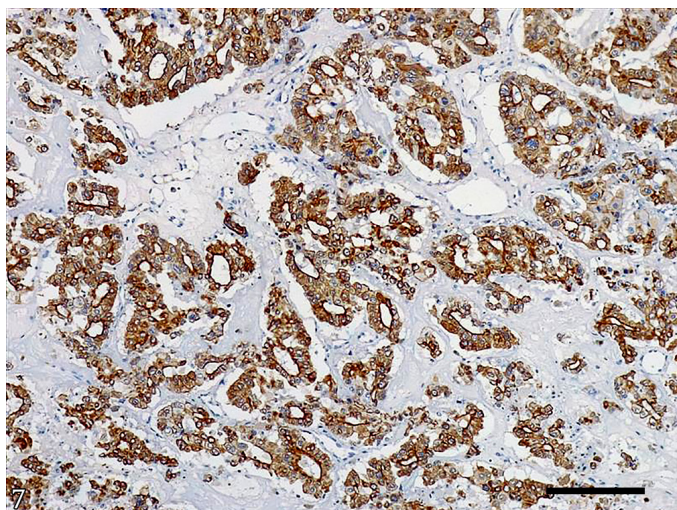


Fig.7. Salivary gland adenocarcinoma, capuchin monkey (*Sapajus nigritus*). Immunohistochemical evaluation with marked and diffuse cytoplasmic staining for anti-CK7 in the epithelial cells. IHC, anti-CK7, DAB, bar = 200 μ m.

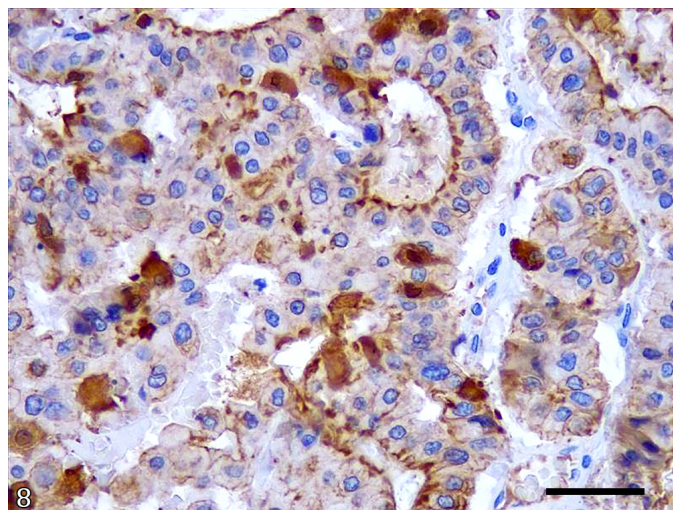


Fig.8. Salivary gland adenocarcinoma, capuchin monkey (*Sapajus nigritus*). Immunohistochemical evaluation with sharp and diffuse cytoplasmic staining for anti-PanCK in the epithelial cells. IHC, anti-PanCK, DAB, bar = 80 μ m.

dysphagia, halitosis, dysphonia, sneezing, difficulty breathing, and choking, among others (Meuten 2017, Howard et al. 2019, Lieske & Rissi 2020). In this presented case, dysphagia and anorexia were a consequence of the tumor formation, reducing the oesophageal lumen and causing lateral displacement. While respiratory difficulty due to tracheal compression was not explicitly mentioned in the clinical history, the presence of pulmonary emphysema suggests potential respiratory challenges.

Salivary gland neoplasms predominantly affect the major glands in dogs and humans, with the submandibular and parotid glands being the most afflicted (Hammer et al. 2001, Ribeiro et al. 2021); in NHP, this similarity is also observed (Howard et al. 2019). In this case, the tumor mass was associated with the submandibular gland, involving the left lateral and medial regions of the neck, making macroscopic observation of the thyroid challenging. The aspiration of neoplastic epithelial cells in the cytology associated with the location of the tumor raised the initial suspicion of thyroid adenocarcinoma, which is more frequent and has more reports in primates than salivary adenocarcinomas.

Histologically, salivary gland neoplasms in humans and other animals are classified into various histological subtypes and by the location of the original neoplastic cells (acini or ducts). The main malignant neoplasms of epithelial origin are adenocarcinomas, acinar cell carcinomas, mucoepidermoid carcinomas, and malignant mixed tumors. However, other subtypes have also been reported: cystadenocarcinoma, myoepithelial carcinoma, squamous cell carcinoma, basal cell adenocarcinoma, and salivary duct carcinoma (Hammer et al. 2001, Meuten 2017, Lieske & Rissi 2020). Among the malignant epithelial neoplasms that affect the salivary gland in NHP, there are four reports of adenocarcinoma, one of undifferentiated carcinoma, one of pleomorphic adenocarcinoma, and one of carcinosarcoma (Howard et al. 2019). The main morphological characteristic of adenocarcinoma is the neoplastic acinar arrangement and the fact that the cells show no characteristics of other histological subtypes, such as the presence of neoplastic

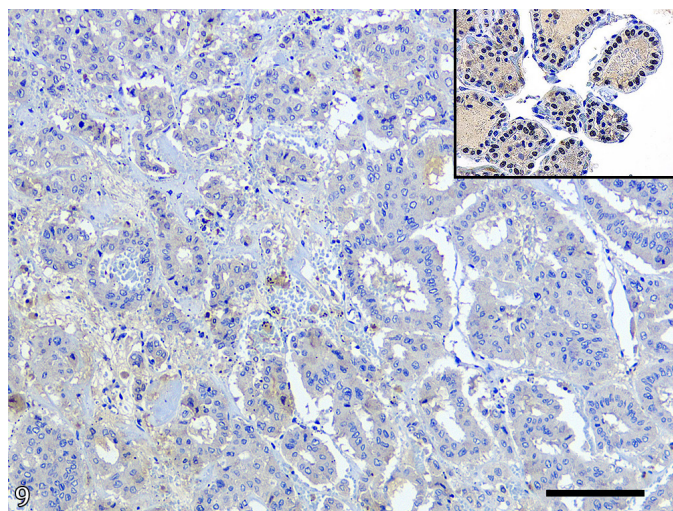


Fig.9. Salivary gland adenocarcinoma, capuchin monkey (*Sapajus nigritus*). Immunohistochemistry revealed no nuclear immunostaining in the neoplastic cells with TTF-1. IHC, anti-TTF-1, DAB, bar = 250 μ m. Inset: Positive control using the *Sapajus nigritus* thyroid gland, showing diffuse and marked nuclear immunostaining in the epithelial cells of thyroid follicles. IHC, anti-TTF-1, DAB.

mesenchymal cells or ductal differentiation (Meuten 2017). The absence of these characteristics leads to the definitive diagnosis of adenocarcinoma.

Initially, determining whether the neoplasm originated in the thyroid or salivary gland was not possible. The histological pattern observed with loss of glandular differentiation confirmed a carcinoma with a high degree of malignancy and aggressive behaviour (Meuten 2017). The absence of colloid reduces the chances of a thyroid neoplasm such as follicular carcinoma, in which follicles filled with colloid are generally formed. Some subtypes of thyroid carcinoma may not have colloid formation, such as the compact type, which has a solid cell pattern (Tochetto et al. 2017); this makes

histological differentiation difficult since, in this case, there were areas showing solid aggregates. Thyroid carcinomas are characterised by cells with “naked” nuclei in the cytology examination (Peleteiro et al. 2011), which were not observed in the aspiration cytology of this case. Another possible differential diagnosis is salivary duct carcinoma. It presents a distinct intraductal neoplastic proliferation with distension of the ducts by neoplastic cells arranged in papillae or a solid form, usually associated with central necrosis (Sozmen et al. 1999, Meuten 2017), which was not observed in this case.

Therefore, an imperative immunohistochemical evaluation was undertaken to discern the cellular origin. The possibility of a thyroid origin was conclusively ruled out through meticulous immunohistochemical scrutiny, revealing the absence of immunolabeling for thyroglobulin and TTF-1. Napsin A is not commonly used as an immunomarker for thyroid-origin neoplasms; however, some thyroid tumors may exhibit positivity (Bishop et al. 2010). Notably, positive labeling for CK7 and Pan CK corroborated an epithelial origin, likely of a glandular nature. Positivity for CK7 is traditionally seen in carcinomas arising from glandular and transitional epithelia, as well as cholangiocarcinomas. Virtually all malignant salivary gland neoplasms exhibit CK7 positivity. Therefore, negativity for this immunomarker effectively excludes salivary gland neoplasms from the differential diagnoses (Nikitakis et al. 2004, Speight & Barrett 2020). In addition, CK20 labelling could be expected in benign or poorly differentiated salivary gland neoplasms (Nikitakis et al. 2004). However, other studies have shown that CK20 is negative in the more undifferentiated cells in human salivary gland neoplasms are, which is an interesting result also observed in our study (CK7 positive and CK20 negative) (Nikitakis et al. 2004). The immunolabeling, combined with the areas of acinar appearance seen on histology and the anatomical location of the neoplasm, supports the diagnosis of salivary gland adenocarcinoma.

Salivary gland carcinomas are usually locally invasive and can lead to metastases in regional lymph nodes and organs, such as the lungs and liver. Although the lung is one of the most metastatic parenchymal organs in dogs, metastasis can affect any organ, from bones to the central nervous system (Habin & Else 1995). The lung is also the site most likely to metastasize in humans due to hematological dissemination (To et al. 2012). We did not observe any nodules or pulmonary alterations that would suggest the presence of metastasis in the macroscopic analysis. However, microscopic evaluation revealed the colonization of neoplastic cells within the parenchyma, thus delineating the presence of pulmonary micrometastasis. The presence of neoplastic cells in the pleural effusion is a consequence of this metastasis in the lung.

CONCLUSION

The definitive diagnosis of salivary gland adenocarcinoma was firmly established based on the comprehensive scrutiny of clinical history, anatomopathological examinations, and immunohistochemical findings related to the neoplasm. This report seems to be the first documentation of a salivary gland adenocarcinoma with lung metastasis in a capuchin monkey, representing a rare occurrence among non-human primates (NHP). We emphasize the importance of performing immunohistochemistry, which was extremely important for the definitive diagnosis and enhanced elucidation of complex cases.

Conflict of interest statement.- The authors declare that there are no conflicts of interest related to this study.

Credit author statement. Alessandra da Cruz: Conceptualization, Methodology, Writing - original draft, Visualization, Investigation. Crisan Smaniotto: Methodology, Writing - Review and Editing. Vinicius Dahm: Methodology, Writing - Review and Editing. Amália Ferronato: Writing - Review and Editing. Manoela Marchezan Piva: Writing - Review and Editing, Conceptualization, Investigation, Supervision. Nelson Dias Lucas: Writing - Review and Editing. Luana Canavessi: Writing - Review and Editing. Laura Formighieri de Noronha: Writing - Review and Editing. Marilene Machado Silva: Writing - Review and Editing. Flávio Shigueru Jojima: Writing - Review and Editing. Aline de Marco Viott: Writing - Review and Editing, Conceptualization, Investigation, Supervision.

Data availability statement.- The data used in this study are available and can be accessed upon request from the corresponding author.

REFERENCES

- American Cancer Society. Salivary gland cancer causes, risk factors, and prevention. 1.800.227.2345. American Cancer Society. Accessed March 18, 2022. <https://www.cancer.org/content/dam/CRC/PDF/Public/8809.00.pdf>
- Bishop JA, Sharma R, Illei PB. Napsin A and thyroid transcription factor-1 expression in carcinomas of the lung, breast, pancreas, colon, kidney, thyroid, and malignant mesothelioma. *Human Pathol* 2010; <https://doi.org/10.1016/j.humpath.2009.06.014>, PMID:19740516
- Cray M, Selmic LE, Ruple A. Salivary neoplasia in dogs and cats: 1996-2017. *Vet Med Sci* 2020; <https://doi.org/10.1002/vms3.228>, PMID:31849188
- Cubas ZS, Silva JCR, Catão-Dias JL. Tratado de animais selvagens: medicina veterinária. 2ª ed. Vol.1. São Paulo: Roca; 2014.
- Habin DJ, Else RW. Parotid salivary gland adenocarcinoma with bilateral ocular and osseous metastasis in a dog. *J Small Anim Pract* 1995; <https://doi.org/10.1111/j.1748-5827.1995.tb02776.x>, PMID:8583760
- Hammer A, Getzy D, Ogilvie G, Upton M, Klausner J, Kisseberth WC. Salivary gland neoplasia in the dog and cat: survival times and prognostic factors. *J Am Anim Hosp Assoc* 2001; <https://doi.org/10.5326/15473317-37-5-478>, PMID:11563448
- Ho K, Lin H, Ann DK, Chu PG, Yen Y. An overview of the rare parotid gland cancer. *Head & Neck Oncol* 2011; <https://doi.org/10.1186/1758-3284-3-40>, PMID:21917153
- Horn-Ross PL, Ljung B-M, Morrow M. Environmental factors and the risk of salivary gland cancer. *Epidemiology* 1997; <https://doi.org/10.1097/00001648-199707000-00011>, PMID:9209856
- Howard E, Gonzalez O, Gumber S, Anderson DC, Kumar S, Dick Jr E. Salivary gland neoplasms in non-human primates: A case series and brief literature review. *J Med Primatol* 2019; <https://doi.org/10.1111/jmp.12412>, PMID:30941779
- Lieske DE, Rissi DR. A retrospective study of salivary gland diseases in 179 dogs (2010-2018). *J Vet Diagn Investig* 2020; <https://doi.org/10.1177/1040638720932169>, PMID:32687011
- Meuten DJ. Tumors in domestic animals. 2017; <https://doi.org/10.1002/9781119181200>
- Miller AD. Neoplasia and proliferative disorders of nonhuman primates, p.325-356. In: Abee CR, Mansfield K, Tardif S, Morris T. Nonhuman primates in biomedical research. 2012. <https://doi.org/10.1016/B978-0-12-381366-4.00006-7>
- Nikitakis NG, Tosios KI, Papanikolaou VS, Rivera H, Papanicolaou SI, Ioffe OB. Immunohistochemical expression of cytokeratins 7 and 20 in malignant salivary gland tumors. *Modern Pathol* 2004; <https://doi.org/10.1038/modpathol.3800064>, PMID:14976534

- Ogawa AI, Takemoto LE, Navarro PL, Hesbiki RE. Salivary gland neoplasms. *Int Arch Otorhinolaryngol* 2008;12(3):409-418.
- Peleteiro MC, Marcos R, Santos M, Correia J, Pissarra H, Carvalho T. Atlas de citologia veterinária. 1ª ed. Lisboa: Lidel; 2011.
- Porcheri C, Mitsiadis TA. Physiology, pathology and regeneration of salivary glands. *Cells* 2019; <https://doi.org/10.3390/cells8090976>, PMID:31455013
- Ribeiro A, Carvalho ALSH, Koth VS, Campos MM. Salivary gland tumors: a ten-year retrospective analysis in a Brazilian teaching hospital. *Revta Bras Cancerol* 2021; <https://doi.org/10.32635/2176-9745.RBC.2021v67n4.1452>
- Schneider AB, Favus MJ, Stachura ME, Arnold MJ, Frohman LA. Salivary gland neoplasms as a late consequence of head and neck irradiation. *Ann Intern Med* 1997; <https://doi.org/10.7326/0003-4819-87-2-160>, PMID:889197
- Sozmen M, Brown PJ, Eveson JW. Salivary duct carcinoma in five cats. *J Comp Pathol* 1999; <https://doi.org/10.1053/jcpa.1999.0329>, PMID:10542121
- Sozmen M, Brown PJ, Eveson JW. Salivary gland basal cell adenocarcinoma: a report of cases in a cat and two dogs. *J Vet Med* 2003; <https://doi.org/10.1046/j.0931.184X.2003.00563.x>, PMID:14633217
- Spangler WL, Culbertson MR. Salivary gland disease in dogs and cats: 245 cases (1985-1988). *J Am Vet Med Assoc* 1991; <https://doi.org/10.2460/javma.1991.198.03.465>, PMID:2010345
- Speight PM, Barrett AW. Salivary gland tumors. *Oral Diseases* 2002; <https://doi.org/10.1034/j.1601-0825.2002.02870.x>, PMID:12363107
- Speight PM, Barrett AW. Salivary gland tumours: diagnostic challenges and an update on the latest WHO classification. *Diagn Histopathol* 2020; <https://doi.org/10.1016/j.mpdhp.2020.01.001>
- To VSH, Chan JYW, Tsang RKY, Wei WI. Review of salivary gland neoplasms. *ISRN Otolaryngol* 2012; <https://doi.org/10.5402/2012/872982>, PMID:23724273
- Tochetto C, Silva TM, Figuera RA, Irigoyen LF, Kommers GD. Neoplasmas da tireoide em cães: 26 casos. *Pesq Vet Bras* 2017; <https://doi.org/10.1590/S0100-736X2017001200016>
- Zachary JF. Pathologic basis of veterinary disease. 6ª ed. St. Louis: Elsevier; 2016.